Closed-form elasticity solution for three-dimensional deformation of functionally graded micro/nano plates on elastic foundation

Abstract

This paper addresses the static deformation of simply supported rectangular micro/nano plates made of functionally graded (FG) materials based on the three-dimensional nonlocal elasticity theory of Eringen. The plates are assumed to be simply supported and rested on a Winkler-Pasternak elastic foundation. Elasticity modulus is assumed to obey an exponential law along the thickness direction of the micro/nano plate. Using the Fourier series, a displacement field is defined that satisfies simply supported boundary condition and reduces three elasticity equations to two independent equations. The closed-form bending response is achieved by exerting boundary conditions of the lateral surfaces. Numerical results are presented to investigate the influences of the gradient index of the material properties, nonlocal parameter and stiffness of elastic foundation on the mechanical behavior of the plates.

H. Salehipour[a]
H. Nahvi[b]*
A.R. Shahidi[c]

Department of Mechanical Engineering, Isfahan University of Technology, Isfahan 8415683111, Iran
[a]h.salehipour@me.iut.ac.ir
[c]shahidi@cc.iut.ac.ir

Corresponding author:
*hnahvi@cc.iut.ac.ir

1 INTRODUCTION

Micro- and nano-scaled plates are very important new type of structures that are utilized in different engineering applications such as micro- and nano-electro mechanical systems (MEMS and NEMS), atomic force microscopes, solar cells and many others. Therefore, to design such structures, their mechanical behaviors such as bending and free and forced vibration should be realized. Recently, FG materials are used in structures such as MEMS and NEMS (Witvrouw et al., 2005; Lee et al., 2006) to increase their thermal resistance. FG materials refer to nonhomogeneous composite materials with smooth and continuous variation of material properties from one surface to the other that is mainly composed of ceramic and metal constituents (Suresh and Mortensen, 1998).

At micrometer and nanometer scale, the effect of van der Waals forces between the atoms becomes important. Since the size effect is not considered in the classical continuum theory, other size-dependent continuum theories such as modified couple stress (Yang et al., 2002), strain gradient (Aifantis, 1999) and nonlocal elasticity (Eringen, 2002) have been developed. Based on size-dependent theories, some works have been carried out to investigate mechanical behavior of micro/nano structures made of FG materials. Lu et al. (2009) considered the surface effects to develop classic and Mindlin plate theories for nano-scaled FG circular films. They evaluated cylindrical bending for simply supported boundary conditions to demonstrate the stability of the developed theories. In another work, Lu et al. (2011) utilized the nonclassical thin plate theory and nonlinear strain of von Karman to solve nonlinear cylindrical bending of simply supported nano-scaled FG rectangular films. Ansari et al. (2011) proposed a size-dependent model for bending and free vibration of Timoshenko microbeams made of FG materials based on the modified strain gradient elasticity theory. Reddy and Kim (2012) presented a nonlinear size-dependent third-order plate theory based on the modified couple stress theory using nonlinear strains of von Karman and power-law distribution for FG material along the thickness direction. They utilized the linear form of this theory to observe mechanical behavior of simply supported rectangular plates (2013). Sharafkhani et al. (2012) obtained mechanical responses of circular FG microplates under nonlinear transverse electrostatic and dynamic forces. They used Galerkin-based step-by-step linearization method to numerically solve the nonlinear governing equations. Natarajan et al. (2012) utilized the numerical method of iso-geometric based finite element to solve nonlocal free flexural vibration of FG nanoplates based on Reissner–Mindlin plate theory. Ke et al. (2012) applied the Hamilton principle and differential quadrature (DQ) method to study size-dependent mechanical behavior of FG annular microplates by incorporating the Mindlin plate theory and modified couple stress theory. Also, Ke et al. (2012) employed the numerical DQ method to investigate nonlinear free vibration of FG Timoshenko microbeams using the modified couple stress theory and von Karman geometric nonlinearity. Shatt et al. (2012; 2013) investigated the surface energy effects with and without the effect of neutral plane position on the static behavior of ultra-thin FG films using Mindlin plate theory. Thai et al. (2013) carried out bending and free vibration of simply supported FG microplates based on the modified couple stress theory. They used Kirchhoff, Mindlin, Reddy and sinusoidal plate theories. Sahmani and Ansari (2013) determined natural frequencies of FG rectangular microplates using third-order shear deformation theory of plate and size-dependent theory of strain gradient. Jung and Han (2013) employed a nonlocal model and used first-order shear deformation theory to study bending and vibration of sigmoid FG nanoplates with simply supported boundary conditions. Hosseini-Hashemi and Nazemnezhad (2013) analytically determined the nonlinear natural frequencies of Euler–Bernoulli microbeams made of FG material in explicit form by the multiple scale method. Hosseini-Hashemi et al. (2013) incorporated Eringen nonlocal elasticity and Mindlin plate theory and presented exact analytical solution for free vibration of circular/annular FG nanoplates with arbitrary boundary conditions. Recently, Salehipour et al. (2015) has presented analytical closed-form solution for free vibration of nonlocal FG plates based on the three-dimensional elasticity theory.

In the present article, using three-dimensional nonlocal elasticity theory of Eringen, exact closed-form solution is derived for cylindrical bending of thick simply supported FG rectangular micro/nano plates resting on Winkler-Pasternak elastic foundations. The variation of material

properties in the thickness direction is based on the exponential law. The closed-form solution is obtained by introducing a displacement field that includes two unknown functions and satisfies edges boundary conditions. Unknown functions are obtained from the governing equations of motion, exerting boundary conditions of the top and bottom surfaces. Numerical examples are presented to examine the influences of the gradient index of the material properties, nonlocal parameter and foundation stiffness on the bending behavior of FG micro/nano plates. The three-dimensional elasticity is an exact theory without any simplicity assumption. The results that obtained by analytical three-dimensional elasticity solution can be used as a benchmark to validate the accuracy of other analytical and numerical methods, which will be developed by researchers in the future.

2 THEORETICAL FORMULATION

Consider a rectangular FG micro/nano plate with a length of a in the x direction, width of b in the y direction and a uniform thickness h in the z direction. Origin of the Cartesian coordinate system $(0; x, y, z)$ is located at a corner of the rectangular plate. The plate is assumed to be simply supported in all edges and attached at the bottom surface to a Winkler-Pasternak elastic foundation.

It is assumed that the material of micro/nano plate is isotropic functionally graded and the Young's modulus varies exponentially from the bottom surface to the top surface as follows

$$E = E_0 \exp(\phi z) \tag{1}$$

where ϕ is the gradient index of the variation and E_0 is Young's modulus at the bottom surface. In addition, Poisson's ratio is assumed to be constant ($\nu = 0.3$). The reason for the choice of exponential law of variation is to be able to obtain analytical solution for three-dimensional elasticity equations. Although the exponential law of variation for FG materials does not exactly reflect any physical reality, but the variation of properties based on this law is similar to some realistic laws such as the power law (for special power indexes).

2.1 Three-dimensional nonlocal equilibrium equations

Nonlocal elasticity theory states that due to the effect of van der Waals forces, the stress at a point in an elastic body depends on the strain at all neighbor points as:

$$\sigma_{ij}(x) = \int_V \gamma(|x - x'|)\sigma_{ij}^l \, \mathrm{d}V(x') \tag{2}$$

where σ_{ij} and σ_{ij}^l are nonlocal and local stresses, respectively, $\gamma(|x - x'|)$ is nonlocal kernel function and $|x - x'|$ denotes the distance between the reference point x and any neighbor point x' in the continuum body. The integral constitutive relation (2) can be represented in a linear differential form (6) as:

$$(1 - \mu \nabla^2)\sigma_{ij} = \sigma_{ij}^l \tag{3}$$

in which $\mu = (e_0 a)^2$ is the nonlocal parameter, e_0 is a material constant evaluated by the experiment and a is an internal characteristic length.

In the absence of body forces, the nonlocal components of stress should satisfy linear three-dimensional elasticity equilibrium equations given as:

$$\sigma_{xx,x} + \sigma_{xy,y} + \sigma_{xz,z} = 0 \tag{4.a}$$

$$\sigma_{xy,x} + \sigma_{yy,y} + \sigma_{yz,z} = 0 \tag{4.b}$$

$$\sigma_{zx,x} + \sigma_{zy,y} + \sigma_{zz,z} = 0 \tag{4.c}$$

The above elasticity equations can be written in terms of the displacement components u, v and w as:

$$G(z)(\nabla^2 u) + \frac{G(z)}{(1-2\nu)}(u_{,xx} + v_{,xy} + w_{,xz}) + G'(z)(u_{,z} + w_{,x}) = 0 \tag{5.a}$$

$$G(z)(\nabla^2 v) + \frac{G(z)}{(1-2\nu)}(u_{,xy} + v_{,yy} + w_{,yz}) + G'(z)(v_{,z} + w_{,y}) = 0 \tag{5.b}$$

$$G(z)(\nabla^2 w) + \frac{G(z)}{(1-2\nu)}(u_{,xz} + v_{,yz} + w_{,zz}) + \frac{2\nu\,G'(z)}{1-2\nu}(u_{,x} + v_{,y} + w_{,z}) + 2G'(z)w_{,z} = 0 \tag{5.c}$$

where $G(z) = E(z)/2(1+\nu)$ is shear modulus and $\nabla^2 = \partial^2/\partial x^2 + \partial^2/\partial y^2 + \partial^2/\partial z^2$.

2.2 Solution procedure

The following displacement field with two unknown functions $\psi_1(z)$ and $\psi_2(z)$ is utilized to solve the governing equations:

$$\begin{Bmatrix} u \\ v \\ w \end{Bmatrix} = \sum_{n=1}^{\infty}\sum_{m=1}^{\infty} \begin{Bmatrix} \psi_1(z)(m\pi/a)\cos(m\pi x/a)\sin(n\pi y/b) \\ \psi_1(z)(n\pi/b)\sin(m\pi x/a)\cos(n\pi y/b) \\ \psi_2(z)\sin(m\pi x/a)\sin(n\pi y/b) \end{Bmatrix} \tag{6}$$

This displacement field satisfies the following boundary conditions of the simply supported plate:

$$\begin{aligned} \sigma_{xx} = v = w = 0, \quad (x = 0, a) \\ \sigma_{yy} = u = w = 0, \quad (y = 0, b) \end{aligned} \tag{7}$$

Substituting displacement field, Eq. (6), and Young's modulus, Eq. (1), into the equilibrium equations, Eqs. (5), leads to just two independent ordinary differential equations with constant coefficients as:

$$G_0 \psi_1''(z) + G_0 \phi \psi_1'(z) - \frac{\lambda_0(1-\nu)}{\nu} \gamma_{mn} \psi_1(z) + \frac{\lambda_0}{2\nu} \psi_2'(z) + G_0 \phi\, \psi_2(z) = 0 \tag{8.a}$$

$$\frac{\lambda_0(1-\nu)}{\nu} \psi_2''(z) + \frac{\lambda_0 \phi(1-\nu)}{\nu} \psi_2'(z) - G_0 \gamma_{mn}\, \psi_2(z) - \frac{\lambda_0}{2\nu} \gamma_{mn}\, \psi_1'(z) - \lambda_0 \phi \gamma_{mn}\, \psi_1(z) = 0 \tag{8.b}$$

where

$$G_0 = \frac{E_0}{2(1+\nu)}, \quad \lambda_0 = \frac{E_0\nu}{(1-2\nu)(1+\nu)} \tag{9}$$

$$\gamma_{mn} = (m\pi/a)^2 + (n\pi/b)^2$$

The solutions of Eqs. (8) are

$$\psi_1(z) = A\exp(\eta z), \qquad \psi_2(z) = B\exp(\eta z) \tag{10}$$

Substituting $\psi_1(z)$ and $\psi_2(z)$ from Eq. (10) into Eqs. (8) and simplifying leads to:

$$\left[G_0\eta^2 + G_0\phi\eta - \frac{\lambda_0(1-\nu)}{\nu}\gamma_{mn} \right]A + \left[\frac{\lambda_0}{2\nu}\eta + G_0\phi \right]B = 0 \tag{11a.}$$

$$\left[-\frac{\lambda_0}{2\nu}\gamma_{mn}\,\eta - \lambda_0\phi\gamma_{mn} \right]A + \left[\frac{\lambda_0(1-\nu)}{\nu}\eta^2 + \frac{\lambda_0\phi(1-\nu)}{\nu}\eta - G_0\gamma_{mn} \right]B = 0 \tag{11.b}$$

From Eqs. (11), characteristic equation is obtained as:

$$\frac{G_0\lambda_0(1-\nu)}{\nu}\eta^4 + \frac{2G_0\lambda_0\phi(1-\nu)}{\nu}\eta^3 + \left[\frac{G_0\lambda_0\phi^2(1-\nu)}{\nu} - G_0^2\gamma_{mn} + \frac{\lambda_0^2(-3+8\nu-4\nu^2)}{4\nu^2}\gamma_{mn} \right]\eta^2$$

$$+ \left\{ -G_0^2\phi\gamma_{mn} - \left[\frac{\lambda_0(1-\nu)}{\nu} \right]^2\phi\gamma_{mn} + \frac{G_0\lambda_0\phi}{2\nu}\gamma_{mn} + \frac{\lambda_0^2\phi}{2\nu}\gamma_{mn} \right\}\eta + \left[\frac{G_0\lambda_0(1-\nu)}{\nu}\gamma_{mn}^2 + G_0\lambda_0\phi^2\gamma_{mn} \right] = 0 \tag{12}$$

The fourth-order characteristic equation (12) have four roots as follows:

$$\begin{Bmatrix} \eta_1 \\ \eta_2 \\ \eta_3 \\ \eta_4 \end{Bmatrix} = -\frac{1}{2}\phi \pm \frac{1}{2}\xi\left[\cos(\theta) \pm j\sin(\theta) \right], \quad j = \sqrt{-1} \tag{13}$$

where

$$\xi = \left[(\phi^2 + 4\gamma_{mn})^2 + \frac{16\phi^2\nu\gamma_{mn}}{1-\nu} \right]^{1/4}$$

$$\theta = \frac{1}{4}Arc\tan\left[\frac{4\phi\sqrt{\nu\gamma_{mn}}}{(\phi^2 + 4\gamma_{mn})\sqrt{1-\nu}} \right] \tag{14}$$

It can be found that the roots of the characteristic equation are complex. Therefore, $\psi_1(z)$ and $\psi_2(z)$ are expressed as:

$$\psi_1(z) = \exp(c_2 z)\big[A_1 \cos(c_1 z) + A_2 \sin(c_1 z)\big] + \exp(c_3 z)\big[A_3 \cos(c_1 z) + A_4 \sin(c_1 z)\big] \tag{15.a}$$

$$\psi_2(z) = \exp(c_2 z)\big[B_1 \cos(c_1 z) + B_2 \sin(c_1 z)\big] + \exp(c_3 z)\big[B_3 \cos(c_1 z) + B_4 \sin(c_1 z)\big] \tag{15.b}$$

where

$$c_1 = \frac{1}{2}\xi \sin(\theta) \tag{16.a}$$

$$\begin{Bmatrix} c_2 \\ c_3 \end{Bmatrix} = -\frac{1}{2}\phi \pm \frac{1}{2}\xi \cos(\theta) \tag{16.b}$$

Moreover, by inserting $\psi_1(z)$ and $\psi_2(z)$ into either of Eqs. (8.a) or (8.b), B_i are obtained in terms of A_i as:

$$
\begin{aligned}
\begin{Bmatrix} B_1 \\ B_2 \end{Bmatrix} &= \frac{1}{d_1^2 + d_2^2}\begin{Bmatrix} (d_1 d_3 + d_2 d_4)A_1 + (d_1 d_4 - d_2 d_3)A_2 \\ (d_2 d_3 - d_1 d_4)A_1 + (d_2 d_4 + d_1 d_3)A_2 \end{Bmatrix} \\
\begin{Bmatrix} B_3 \\ B_4 \end{Bmatrix} &= \frac{1}{f_1^2 + f_2^2}\begin{Bmatrix} (f_1 f_3 + f_2 f_4)A_3 + (f_1 f_4 - f_2 f_3)A_4 \\ (f_2 f_3 - f_1 f_4)A_3 + (f_2 f_4 + f_1 f_3)A_4 \end{Bmatrix}
\end{aligned}
\tag{17}
$$

where

$$
\begin{aligned}
\begin{Bmatrix} d_1 \\ f_1 \end{Bmatrix} &= G_0 \phi + \frac{\lambda_0}{2\nu}\begin{Bmatrix} c_2 \\ c_3 \end{Bmatrix} \\
d_2 = f_2 &= \frac{\lambda_0 c_1}{2\nu} \\
\begin{Bmatrix} d_3 \\ f_3 \end{Bmatrix} &= -G_0 \phi \begin{Bmatrix} c_2 \\ c_3 \end{Bmatrix} - G_0 \begin{Bmatrix} c_2^2 - c_1^2 \\ c_3^2 - c_1^2 \end{Bmatrix} + \frac{\lambda_0(1-\nu)}{\nu}\gamma_{mn} \\
\begin{Bmatrix} d_4 \\ f_4 \end{Bmatrix} &= -G_0 \phi c_1 - 2G_0 \begin{Bmatrix} c_1 c_2 \\ c_1 c_3 \end{Bmatrix}
\end{aligned}
\tag{18}
$$

To obtain unknown coefficients A_i (1, 2, 3, 4), the boundary conditions on the lateral surfaces should be satisfied. The shear stresses on the lateral surfaces are zero, hence,

$$\sigma_{xz} = \sigma_{yz} = 0, \ (z = 0, h) \tag{19}$$

The top surface of the FG micro/nano plate is subjected to the transverse load $Q(x,y)$ and the bottom surface is on an isotropic Winkler-Pasternak elastic foundation. Thus,

$$\sigma_{zz} = k_w w - k_p \left(\frac{\partial^2 w}{\partial x^2} + \frac{\partial^2 w}{\partial y^2}\right), \ (z = 0) \tag{20.a}$$

$$\sigma_{zz} = Q(x,y), \ (z = h) \tag{20.b}$$

where k_w and k_p are the Winkler stiffness and shear stiffness of the foundation, respectively. The stress components σ_{xz}, σ_{yz} and σ_{zz} are obtained from Eqs. (3) and (6) as:

$$\left\{ \begin{array}{c} \sigma_{xz} \\ \sigma_{yz} \end{array} \right\} = \sum_{n=1}^{\infty} \sum_{m=1}^{\infty} \left[\begin{array}{c} U(m\pi/a)\cos(m\pi x/a)\sin(n\pi y/b) \\ V(n\pi/b)\sin(m\pi x/a)\cos(n\pi y/b) \end{array} \right] \tag{21.a}$$

$$\sigma_{zz} = \sum_{n=1}^{\infty} \sum_{m=1}^{\infty} W \sin(m\pi x/a)\sin(n\pi y/b) \tag{21.b}$$

where

$$\left\{ \begin{array}{c} U \\ V \end{array} \right\} = G_0 \left\{ \exp\left[(c_2 + \phi)z\right]\left[K_1 \cos(c_1 z) + K_2 \sin(c_1 z) \right] + \exp\left[(c_3 + \phi)z\right]\left[K_3 \cos(c_1 z) + K_4 \sin(c_1 z) \right] \right\} \tag{22.a}$$

$$W = \frac{\lambda_0}{\nu} \left\{ \exp\left[(c_2 + \phi)z\right]\left[K_5 \cos(c_1 z) + K_6 \sin(c_1 z) \right] + \exp\left[(c_3 + \phi)z\right]\left[K_7 \cos(c_1 z) + K_8 \sin(c_1 z) \right] \right\} \tag{22.b}$$

and

$$\begin{aligned} \left\{ \begin{array}{c} K_1 \\ K_2 \end{array} \right\} &= \frac{1}{g_1^2 + g_2^2} \left\{ \begin{array}{c} (c_2 A_1 + c_1 A_2 + B_1)g_1 + (c_2 A_2 - c_1 A_1 + B_2)g_2 \\ (c_2 A_2 - c_1 A_1 + B_2)g_1 - (c_2 A_1 + c_1 A_2 + B_1)g_2 \end{array} \right\} \\ \left\{ \begin{array}{c} K_3 \\ K_4 \end{array} \right\} &= \frac{1}{g_3^2 + g_4^2} \left\{ \begin{array}{c} (c_3 A_3 + c_1 A_4 + B_3)g_3 + (c_3 A_4 - c_1 A_3 + B_4)g_4 \\ (c_3 A_4 - c_1 A_3 + B_4)g_3 - (c_3 A_3 + c_1 A_4 + B_3)g_4 \end{array} \right\} \end{aligned} \tag{23.a}$$

$$\begin{aligned} \left\{ \begin{array}{c} K_5 \\ K_6 \end{array} \right\} &= \frac{1}{g_1^2 + g_2^2} \left\{ \begin{array}{c} \left[(1-\nu)(c_2 B_1 + c_1 B_2) - \nu\gamma_{mn}A_1\right]g_1 + \left[(1-\nu)(c_2 B_2 - c_1 B_1) - \nu\gamma_{mn}A_2\right]g_2 \\ \left[(1-\nu)(c_2 B_2 - c_1 B_1) - \nu\gamma_{mn}A_2\right]g_1 - \left[(1-\nu)(c_2 B_1 + c_1 B_2) - \nu\gamma_{mn}A_1\right]g_2 \end{array} \right\} \\ \left\{ \begin{array}{c} K_7 \\ K_8 \end{array} \right\} &= \frac{1}{g_3^2 + g_4^2} \left\{ \begin{array}{c} \left[(1-\nu)(c_3 B_3 + c_1 B_4) - \nu\gamma_{mn}A_3\right]g_3 + \left[(1-\nu)(c_3 B_4 - c_1 B_3) - \nu\gamma_{mn}A_4\right]g_4 \\ \left[(1-\nu)(c_3 B_4 - c_1 B_3) - \nu\gamma_{mn}A_4\right]g_3 - \left[(1-\nu)(c_3 B_3 + c_1 B_4) - \nu\gamma_{mn}A_3\right]g_4 \end{array} \right\} \end{aligned} \tag{23.b}$$

$$\begin{aligned} \left\{ \begin{array}{c} g_1 \\ g_3 \end{array} \right\} &= 1 + \mu\gamma_{mn} - \mu \left\{ \begin{array}{c} (c_2 + \phi)^2 - c_1^2 \\ (c_3 + \phi)^2 - c_1^2 \end{array} \right\} \\ \left\{ \begin{array}{c} g_2 \\ g_4 \end{array} \right\} &= 2\mu \left\{ \begin{array}{c} c_1(c_2 + \phi) \\ c_1(c_3 + \phi) \end{array} \right\} \end{aligned} \tag{23.c}$$

Using Eqs. (21.a) and (21.b), the four shear boundary equations, Eq. (19), reduce to two independent equations as follows:

$$\begin{aligned} &\exp\left[(c_2 + \phi)z\right]\left[K_1 \cos(c_1 z) + K_2 \sin(c_1 z) \right] + \\ &\exp\left[(c_3 + \phi)z\right]\left[K_3 \cos(c_1 z) + K_4 \sin(c_1 z) \right] = 0, \quad (z = 0, h) \end{aligned} \tag{24}$$

Also, the two boundary equations (20.a) and (20.b), lead to the following algebraic equations:

$$\begin{aligned} &\frac{\lambda_0}{\nu} \left\{ \exp\left[(c_2 + \phi)z\right]\left[K_5 \cos(c_1 z) + K_6 \sin(c_1 z) \right] + \exp\left[(c_3 + \phi)z\right]\left[K_7 \cos(c_1 z) + K_8 \sin(c_1 z) \right] \right\} = \\ &\left\{ k_w + k_p \left[(m\pi/a)^2 + (n\pi/b)^2 \right] \right\} \psi_2(0), \quad (z = 0) \end{aligned} \tag{25.a}$$

$$\begin{aligned} &\frac{\lambda_0}{\nu} \left\{ \exp\left[(c_2 + \phi)z\right]\left[K_5 \cos(c_1 z) + K_6 \sin(c_1 z) \right] + \\ &\exp\left[(c_3 + \phi)z\right]\left[K_7 \cos(c_1 z) + K_8 \sin(c_1 z) \right] \right\} = Q_{mn}, \quad (z = h) \end{aligned} \tag{25.b}$$

where

$$Q_{mn} = \frac{4}{ab} \int_0^b \int_0^a Q(x,y) \sin(m\pi x/a) \sin(n\pi y/b) dx dy \tag{26}$$

The solution is completed by obtaining the constant coefficients A_1, A_2, A_3 and A_4 from the four algebraic equations (24) and (25).

3   NUMERICAL RESULTS AND DISCUSSION

For the simplicity and without loss of generality, in all examples it is assumed that the transverse loading has one of the following sinusoidal or uniform forms:

$$Q(x,y) = -q\sin(\pi x/a)\sin(\pi y/b) \tag{27.a}$$

$$Q(x,y) = -q \tag{27.b}$$

The following dimensionless forms of the displacements, stresses, nonlocal parameter, gradient index of the material properties and foundation parameters are utilized in the numerical examples:

$$\bar{u} = G_0 u/qh, \quad \bar{v} = G_0 v/qh, \quad \bar{w} = G_0 w/qh \tag{28.a}$$

$$\bar{\sigma}_{ij} = \sigma_{ij}/q \tag{28.b}$$

$$K_W = k_w a^4/D, \quad K_p = k_p a^2/D \tag{28.c}$$

$$\bar{\phi} = E_h/E_0 = \exp(\phi h), \quad \bar{\mu} = \mu/h^2 \tag{28.d}$$

where $D = G_0 h^3/6(1-\nu)$ is a reference of the bending rigidity of the plate.

No results have been published for bending response of micro/nano FG plates with exponential variation of material properties based on the nonlocal elasticity. Thus, the comparison study is presented for local FG plates and nonlocal homogeneous plates. Table 1 compares the central out-of-plane displacement of a thick square local FG plate, $G_h w/qh$, with the results given by Kashtalyan (2004). The results are presented for the length-to-thickness ratio of 3 ($a/h = 3$) and a range of the inhomogeneity gradient index ($\ln(E_h/E_0)$), where G_h and E_h denote shear modulus and Young's modulus of the top surface of the plate. Excellent agreement is observed between the results.

In Table 2, the central out-of-plane displacement of a square local homogeneous plate on Winkler-Pasternak elastic foundation is compared with the results given by Huang et al. (2008). The results are presented for different stiffness values of foundation. Excellent agreement is observed between the results.

The central out-of-plane displacement of a square nonlocal homogeneous plate is tabulated in Table 3 and compared with the results obtained by two-dimensional Third-order plate theory (Aghababaei and Reddy, 2009) for different values of nonlocal parameter.

Inhomogeneity $\ln(E_h/E_0)$	Method	$\dfrac{G_h w}{qh}\left(\dfrac{a}{2},\dfrac{a}{2},\dfrac{h}{2}\right)$
10^{-1}	Kashtalyan (2004)	-1.41464
	Present	-1.414636
10^{-2}	Kashtalyan (2004)	-1.34960
	Present	-1.349603
10^{-3}	Kashtalyan (2004)	-1.34326
	Present	-1.343258
10^{-4}	Kashtalyan (2004)	-1.34263
	Present	-1.342625
10^{-5}	Kashtalyan (2004)	-1.34256
	Present	-1.342562
10^{-6}	Kashtalyan (2004)	-1.34256
	Present	-1.342555

Table 1: Comparison of normalized out-of-plane displacement $G_h w/(qh) = f\left(a/2, a/2, h/2\right)$ for a square FG plate with $a/h = 3$, subjected to a sinusoidal load q.

K_W	K_P	Method	$-10^3 \times \dfrac{E_0 h^3 w}{12(1-\nu^2)qa^4}\left(\dfrac{a}{2},\dfrac{a}{2},\dfrac{h}{2}\right)$
1	1	Huang et al. (2008)	3.8546
		Present (100 term series)	3.85495
	3^4	Huang et al. (2008)	0.7630
		Present (100 term series)	0.76314
	5^4	Huang et al. (2008)	0.1153
		Present (100 term series)	0.11539
3^4	1	Huang et al. (2008)	3.2105
		Present (100 term series)	3.21084
	3^4	Huang et al. (2008)	0.7317
		Present (100 term series)	0.73189
	5^4	Huang et al. (2008)	0.1154
		Present (100 term series)	0.11461
5^4	1	Huang et al. (2008)	1.4765
		Present (100 term series)	1.47673
	3^4	Huang et al. (2008)	0.5704
		Present (100 term series)	0.57052
	5^4	Huang et al. (2008)	0.1095
		Present (100 term series)	0.10955

Table 2: Comparison of normalized out-of-plane displacement $\left(-10^3 \times E_0 h^3 w/\left[12(1-\nu^2)qa^4\right] = f\left(a/2, a/2, h/2\right)\right)$ for a square local homogeneous plate with $a/h = 100$, subjected to a uniform load q resting on Winkler-Pasternak elastic foundation.

Dimensionless Nonlocal parameter	Method	$-10^2 \times \dfrac{E_0 h^3 w}{qa^4}\left(\dfrac{a}{2},\dfrac{a}{2},\dfrac{h}{2}\right)$
0	Aghababaei and Reddy (2009)	4.1853
	Present (100 term series)	4.6401
0.5	Aghababaei and Reddy (2009)	4.5607
	Present (100 term series)	5.2221
1	Aghababaei and Reddy (2009)	4.9362
	Present (100 term series)	5.8041
1.5	Aghababaei and Reddy (2009)	5.3116
	Present (100 term series)	6.3861
2	Aghababaei and Reddy (2009)	5.6871
	Present (100 term series)	6.9681

Table 3: Comparison of normalized out-of-plane displacement ($-10^2 \times E_0 h^3 w/(qa^4) = f(a/2, a/2, h/2)$) for a square nonlocal homogeneous plate with $a/h = 10$, subjected to a uniform load q.

Through-thickness variations of the dimensionless longitudinal displacement, $\bar{u}(0, a/2, z)$, and dimensionless transverse displacement, $\bar{w}(a/2, a/2, z)$, in a square FG micro/nano plate on elastic foundation with the length-to-thickness ratio of 5 ($a/h = 5$) are illustrated in Figures 1 and 2, respectively. Results are shown for the dimensionless gradient index $\bar{\phi}$ of 1 and 5, dimensionless nonlocal parameter $\bar{\mu}$ of 0 and 1, and different values of foundation stiffnesses. It is noticiable that the results of Figures 1-6 are for the case of transverse sinusoidal loading.

By comparing the results of Figures 1a and 1b, and also Figures 2a and 2b, it can be observed that the absolute longitudinal displacement of the local FG plate is higher than that of the isotropic one while, the absolute transverse displacement is lower. Moreover, from Figures 1a and 1c, and also Figs. 2a and 2c, it can be seen that the absolute longitudinal displacement of the nonlocal isotropic plate is lower than that of the local isotropic plate, whereas the absolute transverse displacement is higher. It can be concluded from Figures 1a-c and 2a-c that by increasing the foundation stiffness, the absolute longitudinal and transverse displacements, and also their through-thickness variation slopes decrease. But, for the nonlocal FG plate with $\bar{\phi} = 5$ and $\bar{\mu} = 1$, increasing the foundation stiffness decreases the stiffness of the structure. Dissimilar results of Figures 1d and 2d are due to the fact that in the nonlocal elasticity theory Laplace operator ∇^2 exerts on both the material properties and displacement components.

Figures 3-6 show through-thickness distribution of dimensionless in-plane and out-of-plane stress components, $\bar{\sigma}_{ij}$, in a square FG micro/nano plate ($a/h = 5$) with different elastic foundation values. It can be seen from Figures 3 and 4 that the through-thickness distribution of in-plane stresses $\bar{\sigma}_{xy}$ and $\bar{\sigma}_{xx}$ for the local and nonlocal FG plates, contrary to the local isotropic and nonlocal plates, are nonlinear. Moreover, it is deduced from Figures 3-6 that the through-thickness distribution of stress components are the same for the local and nonlocal isotropic plates, and also for the local and nonlocal FG plates, without elastic foundation.
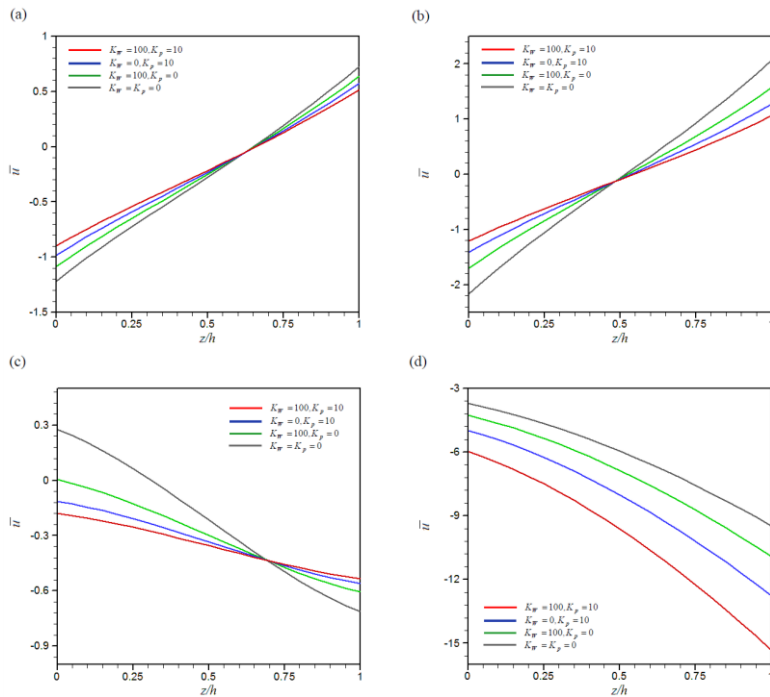
Figure 1: Through-thickness variation of the dimensionless longitudinal displacement, $\bar{u}(0, a/2, z)$, for different values of foundation stiffness, (a) local isotropic plate with $\bar{\phi} = 0$, $\bar{\mu} = 0$; (b) local FG plate with $\bar{\phi} = 5$, $\bar{\mu} = 0$; (c) nonlocal isotropic plate with $\bar{\phi} = 0$, $\bar{\mu} = 1$; (d) nonlocal FG plate with $\bar{\phi} = 5$, $\bar{\mu} = 1$.
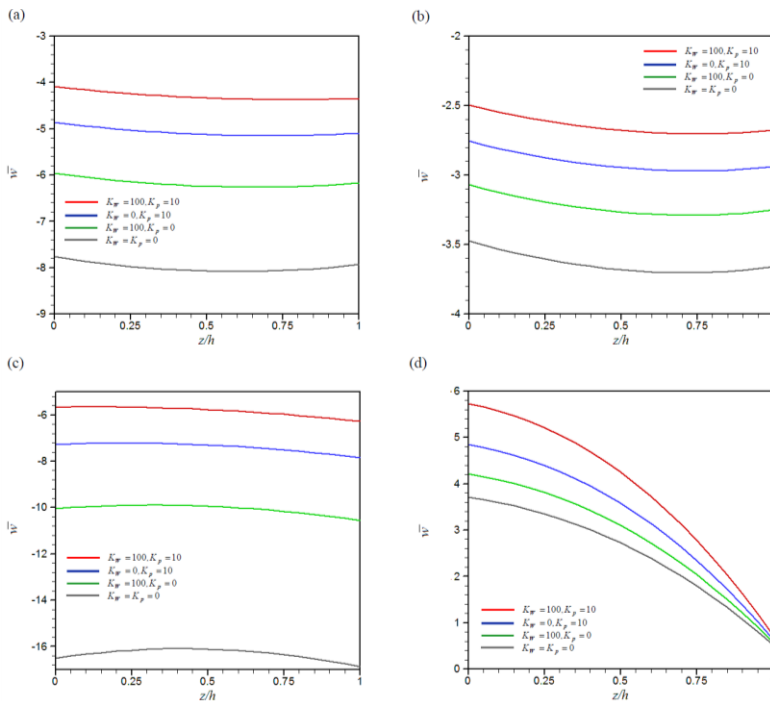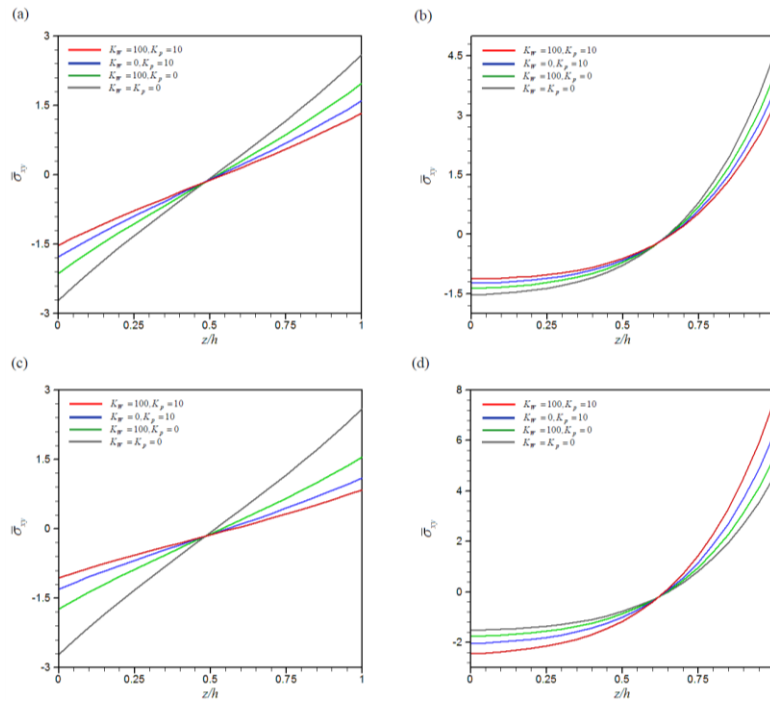

Figure 2: Through-thickness variation of the dimensionless transverse displacement, $\bar{w}(a/2, a/2, z)$, for different values of foundation stiffness, (a) local isotropic plate with $\bar{\phi} = 0$, $\bar{\mu} = 0$; (b) local FG plate with $\bar{\phi} = 5$, $\bar{\mu} = 0$; (c) nonlocal isotropic plate with $\bar{\phi} = 0$, $\bar{\mu} = 1$; (d) nonlocal FG plate with $\bar{\phi} = 5$, $\bar{\mu} = 1$.
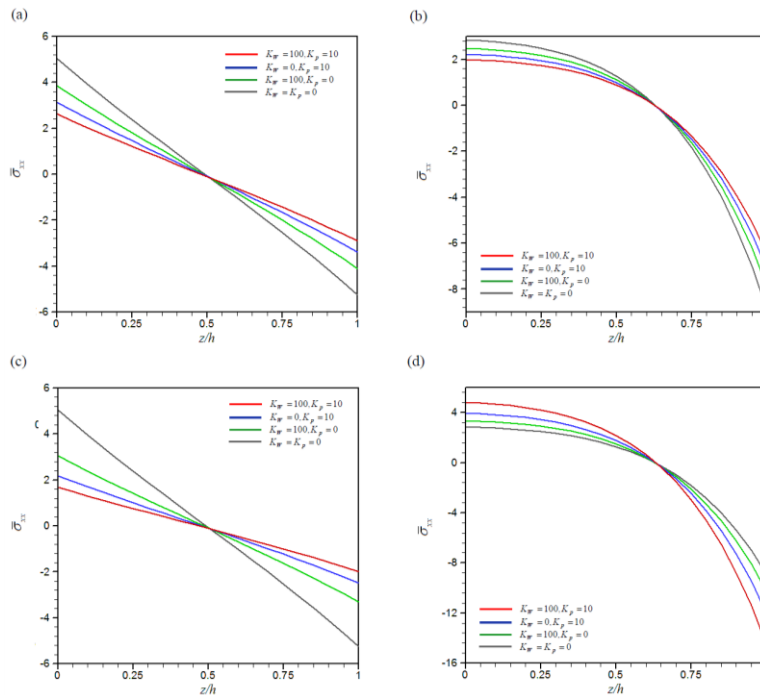
Figure 3: Through-thickness variation of the dimensionless in-plane shear stress, $\bar{\sigma}_{xy}(0,0,z)$, for different values of foundation stiffness, (a) local isotropic plate with $\bar{\phi} = 0$, $\bar{\mu} = 0$; (b) local FG plate with $\bar{\phi} = 5$, $\bar{\mu} = 0$; (c) nonlocal isotropic plate with $\bar{\phi} = 0$, $\bar{\mu} = 1$; (d) nonlocal FG plate with $\bar{\phi} = 5$, $\bar{\mu} = 1$.

Figure 4: Through-thickness variation of the dimensionless longitudinal normal stress, $\bar{\sigma}_{xx}(a/2, a/2, z)$, for different values of foundation stiffness, (a) local isotropic plate with $\bar{\phi} = 0$, $\bar{\mu} = 0$; (b) local FG plate with $\bar{\phi} = 5$, $\bar{\mu} = 0$; (c) nonlocal isotropic plate with $\bar{\phi} = 0$, $\bar{\mu} = 1$; (d) nonlocal FG plate with $\bar{\phi} = 5$, $\bar{\mu} = 1$.
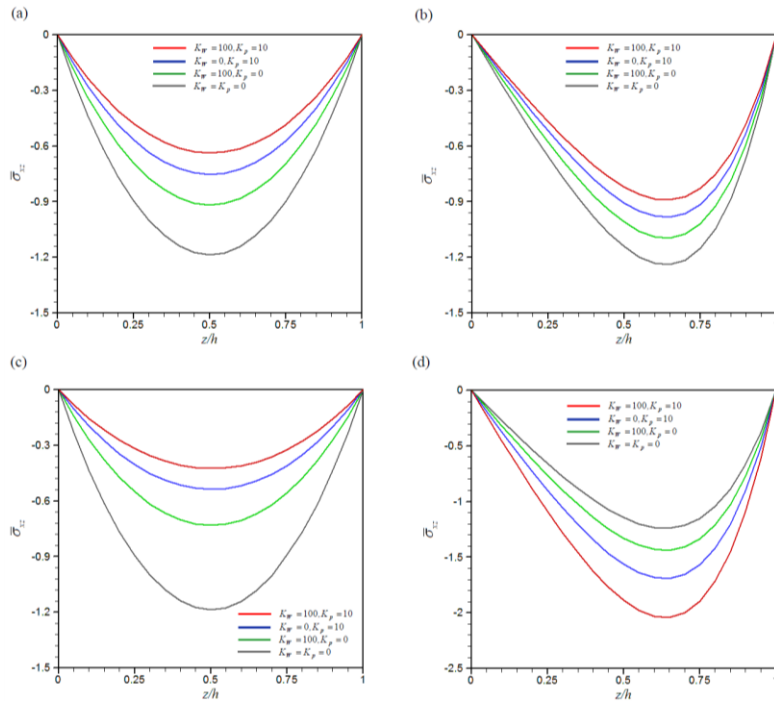
Figure 5: Through-thickness variation of the dimensionless transverse shear stress, $\bar{\sigma}_{xz}(0, a/2, z)$, for different values of foundation stiffness, (a) local isotropic plate with $\bar{\phi} = 0, \bar{\mu} = 0$; (b) local FG plate with $\bar{\phi} = 5, \bar{\mu} = 0$; (c) nonlocal isotropic plate with $\bar{\phi} = 0, \bar{\mu} = 1$; (d) nonlocal FG plate with $\bar{\phi} = 5, \bar{\mu} = 1$.
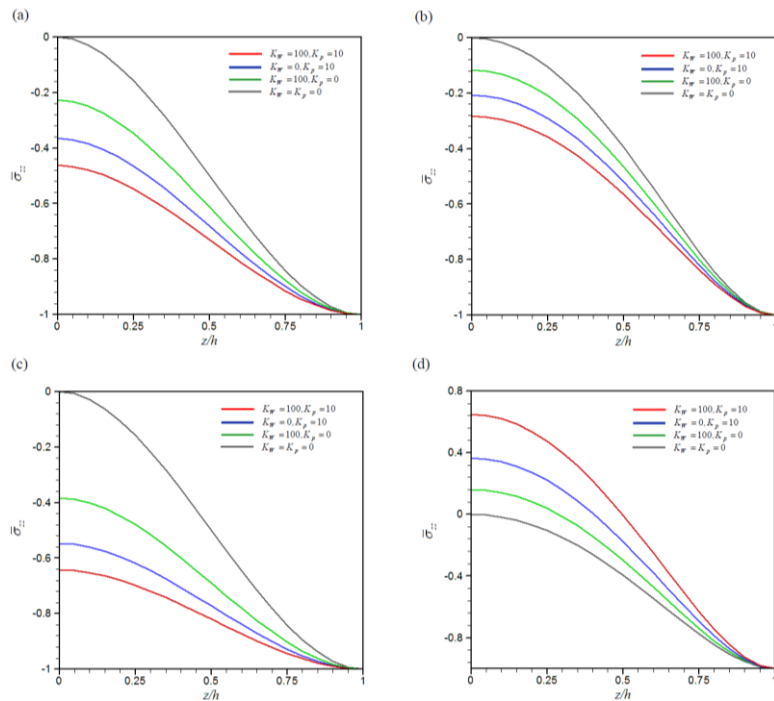

Figure 6: Through-thickness variation of the dimensionless transverse normal stress, $\bar{\sigma}_{zz}(a/2, a/2, z)$, for different values of foundation stiffness, (a) local isotropic plate with $\bar{\phi} = 0, \bar{\mu} = 0$; (b) local FG plate with $\bar{\phi} = 5, \bar{\mu} = 0$; (c) nonlocal isotropic plate with $\bar{\phi} = 0, \bar{\mu} = 1$; (d) nonlocal FG plate with $\bar{\phi} = 5, \bar{\mu} = 1$.

For nonzero values of foundation stiffness, the absolute values of the in-plane stress components $\bar{\sigma}_{xy}$ and $\bar{\sigma}_{xx}$, and the absolute value of shear stress $\bar{\sigma}_{xz}$ of the local isotropic plate are higher than those of the nonlocal isotropic one while, the normal transverse stress $\bar{\sigma}_{zz}$ has opposite results. From Figures 3-6, it is observed that the values of the stress component at a certain dimensionless coordinate z/h are independent of the foundation stiffness value. The mentioned coordinate for the in-plane stress components $\bar{\sigma}_{xy}$ and $\bar{\sigma}_{xx}$ is on the neutral plane whose position varies with the gradient index value of the material properties. It is obvious that except for the nonlocal FG plate ($\bar{\phi} = 5$, $\bar{\mu} = 1$), increasing the stiffness foundation decreases the absolute values of the in-plane and out-of-plane stress components. For the case of the nonlocal FG plate with $\bar{\phi} = 5$ and $\bar{\mu} = 1$, the absolute values of the in-plane and out-of-plane stress components increase when the foundation stiffness increases. As mentioned, this is attributed to the effect of Laplace operator ∇^2 in the nonlocal elasticity theory.

4   CONCLUSION

In this work, a closed-form nonlocal solution for bending of simply-supported FG micro/nano plates, under transverse load, is presented based on the three dimensional elasticity. Plates are assumed to be rested on a Winkler-Pasternak elastic foundation. Variation of the elasticity modulus in the thickness direction is assumed to be exponential, while the Poisson's ratio is considered to be constant. The through-thickness distribution of the displacement and stress fields are studied for different values of the nonlocal parameter, gradient index of material properties and foundation stiffness. The following noticeable conclusions are obtained from the results:

- The absolute transverse displacement of the local isotropic plate is higher than that of the local FG plate while, it is lower than that of the nonlocal isotropic plate.
- The through-thickness variations of stress components are the same for the cases of the local isotropic and nonlocal plates, and also for the local and nonlocal FG plates, without elastic foundation.
- Stress components are independent of the foundation stiffness for certain values of dimensionless z coordinate.
- For the local and nonlocal isotropic plates, and local FG plates, increasing the foundation stiffness decreases the absolute displacements and the stress components values.
- For the nonlocal FG case, by increasing the foundation stiffness, the transverse displacement increases, which is the opposite what was expected. This is attributed to the effect of Laplace operator ∇^2 in the nonlocal elasticiti theory.

References

Aifantis, E.C., (1999). Strain gradient interpretation of size effects. Int. J. Fractures 95: 1-4.

Aghababaei, R., Reddy, J.N., (2009). Nonlocal third-order shear deformation plate theory with application to bending and vibration of plates. Journal of Sound and Vibration 326: 277-289.

Ansari, R., Gholami, R., Sahmani, S., (2011). Free vibration analysis of size-dependent functionally graded microbeams based on the strain gradient Timoshenko beam theory. Composite Structures 94: 221–228.

Eringen, A.C., (2002). Nonlocal continuum field theories. Springer, New York.

Hosseini-Hashemi, Sh., Bedroud, M., Nazemnezhad, R., (2013). An exact analytical solution for free vibration of functionally graded circular/annular Mindlin nanoplates via nonlocal elasticity. Composite Structures 103: 108–118.

Hosseini-Hashemi, Sh., Nazemnezhad, R., (2013). An analytical study on the nonlinear free vibration of functionally graded nanobeams incorporating surface effects. Composites Part B 52: 199–206.

Huang, Z.Y., Lu, C.F., Chen, W.Q., (2008). Benchmark solutions for functionally graded thick plates resting on Winkler–Pasternak elastic foundations. Composite Structures 85: 95-104.

Jung, W.Y., Han, S.C., (2013) Analysis of sigmoid functionally graded material (S-FGM) nanoscale plates using the nonlocal elasticity theory. Journal of Mathematical Problems in Engineering 49: 449-458.

Kashtalyan, M., (2004). Three-dimensional elasticity solution for bending of functionally graded rectangular plates. European Journal Mechanics and Solids 23: 853-864.

Ke, L.L., Wang, Y.S., Yang, J., Kitipornchai, S., (2012). Nonlinear free vibration of size-dependent functionally graded microbeams. International Journal of Engineerng Science 50: 256–67.

Ke, L.L., Yang, J., Kitipornchai, S., Bradford, M.A., (2012). Bending, buckling and vibration of size-dependent functionally graded annular microplates. Composite Structures 94: 3250-3257.

Kim, J., Reddy, J.N., (2013). Analytical solutions for bending, vibration, and buckling of FGM plates using a couple stress-based third-order theory. Composite Structures 103: 86-98.

Lee, Z., Ophus, C., Fischer, L.M., Nelson-Fitzpatrick, N., Westra, K.L., Evoy, S., et al., (2006). Metallic NEMS components fabricated from nanocomposite Al–Mo films. Nanotechnology 17: 3063-3070.

Lu, C.F., Chen, W.Q., Lim, C.W., (2009). Elastic mechanical behavior of nano-scaled FGM films incorporating surface energies. Journal of Composite Science and Thechnology 69: 1124-30.

Lu, C.F., Chen, W.Q., Lim, C.W., (2009). Size-dependent elastic behavior of FGM ultra-thin films based on generalized refined theory. International Journal of Solids and Structures 46: 1176-1185.

Lu, C.F., Wu, D.Z., Chen, W.Q., (2011). Nonlinear responses of nanoscale FGM films including the effects of surface energies. Transactions on Nanotechology 10: 1321-1327.

Natarajan, S., Chakraborty, S., Thangavel, M., Bordas, S., Rabczuk, T., (2012). Size-dependent free flexural vibration behavior of functionally graded nanoplates. Computational Materials Science 65: 74-80.

Reddy, J.N., Kim, J., (2012). A nonlinear modified couple stress-based third-order theory of functionally graded plates. Composite Structures 94: 1128-1143.

Sahmani, S., Ansari, R., (2013). On the free vibration response of functionally graded higher-order shear deformable microplates based on the strain gradient elasticity theory. Composite Structures 95: 430–442.

Salehipour, H., Nahvi, H., Shahidi, A.R., (2015). Exact analytical solution for free vibration of functionally graded micro/nanoplates via three-dimensional nonlocal elasticity. Physica E 66: 350–358.

Shaat, M., Mahmoud, F.F., Alshorbagy, A.E., Alieldin, S.S., Meletis, E.I., (2013). Bending analysis of ultra-thin functionally graded Mindlin plates incorporating surface energy effects. International Journal of Mechanical Science 75: 223–232.

Shaat, M., Mahmoud, F.F., Alshorbagy, A.E., Alieldin, S.S., Meletis, E.I., (2012). Size-dependent analysis of functionally graded ultra-thin films. Structural Engineering and Mechanics 43: 431–448.

Sharafkhani, N., Rezazadeh, G.H., Shabani, R., (2012). Study of mechanical behavior of circular FGM microplates under nonlinear electrostatic and mechanical shock loadings. Acta Mechanica 223: 579-591.

Suresh, S., Mortensen, A., (1998). Fundamentals of functionally graded materials. UK: IOM Communications, London.

Thai, H-T., Choi, D-H., (2013). Size-dependent functionally graded Kirchhoff and Mindlin plate models based on a modified couple stress theory. Composite Structures 95: 142-153.

Thai, H-T., Kim, S-E., (2013). A size-dependent functionally graded Reddy plate model based on a modified couple stress theory. Composites Part B 50: 1636-1645.

Thai, H-T., Vo, T.P., (2013). A size-dependent functionally graded sinusoidal plate model based on a modified couple stress theory. Composite Structures 96: 376–383.

Witvrouw, A., Mehta, A., (2005). The use of functionally graded poly-SiGe layers for MEMS applications. Materials Science Forum 492-493: 255-260.

Yang, F., Chong, A.C.M., Lam, D.C.C., Tong, P., (2002). Couple stress based strain gradient theory for elasticity. International Journal of Solids and Struct 39: 2731-43.